Wide Temperature Magnetization Characteristics of Transverse Magnetically Annealed Amorphous Tapes for High Frequency Aerospace Magnetics

Janis M. Niedra
Dynacs Engineering Company, Inc., Cleveland, Ohio

Gene E. Schwarze
Glenn Research Center, Cleveland, Ohio

The NASA STI Program Office . . . in Profile

Since its founding, NASA has been dedicated to the advancement of aeronautics and space science. The NASA Scientific and Technical Information (STI) Program Office plays a key part in helping NASA maintain this important role.

The NASA STI Program Office is operated by Langley Research Center, the Lead Center for NASA's scientific and technical information. The NASA STI Program Office provides access to the NASA STI Database, the largest collection of aeronautical and space science STI in the world. The Program Office is also NASA's institutional mechanism for disseminating the results of its research and development activities. These results are published by NASA in the NASA STI Report Series, which includes the following report types:

- TECHNICAL PUBLICATION. Reports of completed research or a major significant phase of research that present the results of NASA programs and include extensive data or theoretical analysis. Includes compilations of significant scientific and technical data and information deemed to be of continuing reference value. NASA's counterpart of peer-reviewed formal professional papers but has less stringent limitations on manuscript length and extent of graphic presentations.

- TECHNICAL MEMORANDUM. Scientific and technical findings that are preliminary or of specialized interest, e.g., quick release reports, working papers, and bibliographies that contain minimal annotation. Does not contain extensive analysis.

- CONTRACTOR REPORT. Scientific and technical findings by NASA-sponsored contractors and grantees.

- CONFERENCE PUBLICATION. Collected papers from scientific and technical conferences, symposia, seminars, or other meetings sponsored or cosponsored by NASA.

- SPECIAL PUBLICATION. Scientific, technical, or historical information from NASA programs, projects, and missions, often concerned with subjects having substantial public interest.

- TECHNICAL TRANSLATION. English-language translations of foreign scientific and technical material pertinent to NASA's mission.

Specialized services that complement the STI Program Office's diverse offerings include creating custom thesauri, building customized data bases, organizing and publishing research results . . . even providing videos.

For more information about the NASA STI Program Office, see the following:

- Access the NASA STI Program Home Page at *http://www.sti.nasa.gov*

- E-mail your question via the Internet to help@sti.nasa.gov

- Fax your question to the NASA Access Help Desk at (301) 621-0134

- Telephone the NASA Access Help Desk at (301) 621-0390

- Write to:
  NASA Access Help Desk
  NASA Center for AeroSpace Information
  7121 Standard Drive
  Hanover, MD 21076

Wide Temperature Magnetization Characteristics of Transverse Magnetically Annealed Amorphous Tapes for High Frequency Aerospace Magnetics

Janis M. Niedra
Dynacs Engineering Company, Inc., Cleveland, Ohio

Gene E. Schwarze
Glenn Research Center, Cleveland, Ohio

National Aeronautics and
Space Administration

Glenn Research Center

August 1999

Acknowledgments

WIDE TEMPERATURE MAGNETIZATION CHARACTERISTICS OF TRANSVERSE MAGNETICALLY ANNEALED AMORPHOUS TAPES FOR HIGH FREQUENCY AEROSPACE MAGNETICS

Janis M. Niedra
Dynacs Engineering Co., Inc.
NASA Glenn Research Center Group
Cleveland, Ohio 44135

Gene E. Schwarze
NASA Glenn Research Center
Cleveland, Ohio 44135

ABSTRACT

100 kHz magnetization properties of sample transverse magnetically annealed, cobalt-based amorphous and iron-based nanocrystalline tape wound magnetic cores are presented over the temperature range of −150 C to 150 C, at selected values of B_{peak}. Frequency resolved characteristics are given over the range of 50 kHz to 1 MHz, but at B_{peak} =0.1 T and 50 C only. Basic exciting winding current and induced voltage data were taken on bare toroidal cores, in a standard type measurement setup. A linear permeability model, which represents the core by a parallel L-R circuit, is used to interpret and present the magnetization characteristics and several figures of merit applicable to inductor materials are reviewed.. The 100 kHz permeability thus derived decreases with increasing temperature for the Fe-based, nanocrystalline material, but increases roughly linearly with temperature for the two Co-based materials, as long as B_{peak} is sufficiently low to avoid saturation effects. Due to the high permeabilities, rather low values of the 'quality factor' Q, from about 20 to below unity, were obtained over the frequency range of 50 kHz to 1 MHz (50 C, B_{peak}=0.1 T). Therefore these cores must be gapped in order to make up high Q or high current inductors. However, being rugged, low core loss materials with flat B-H loop characteristics, they may provide new solutions to specialty inductor applications.

INTRODUCTION

It is well known [1] that the B-H characteristics of amorphous ribbons of certain metallic alloys, usually based on Co and/or Fe, can be controlled from highly square to linear by magnetic anneal and, in some cases, in combination with partial recrystallization [2, 3]. Moreover, these ribbons exhibit a very low and generally temperature insensitive core loss [4], that is as low as that of the best ferrites in say the 100 to 500 kHz frequency range.

The particular amorphous tapes measured here have been annealed to linearize as much as possible their B-H characteristics and possibly also to lower their permeability μ. A lower μ can increase the quality factor

'Q' of an inductor, as will be explained, and is desirable to avoid magnetic saturation in a high current inductor. Commercial cores wound with these specially annealed amorphous tapes serve well in common mode choke and flux ratcheting resistant, high frequency transformer applications. These applications benefit from the very low core loss, high permeability, near zero saturation magnetostriction and very high plastic yield strength of such tapes. If the effective permeability can be controlled, then these tapes would also be candidates for high frequency power inductors in aerospace applications. Accordingly, this paper presents the high frequency magnetization and energy storage properties of the same cores whose core loss properties are given in reference [4].

100 kHz magnetization properties of two cobalt-based amorphous tape wound cores and one iron-based, nanocrystalline tape wound core are presented over the temperature range of −150 C to 150 C, at selected peak B-fields (B_{peak}, or B_p). Frequency resolved characteristics are given over the range of 50 kHz to 1 MHz, but at B_{peak} =0.1 T and 50 C only. Although not exhaustive, this data provides a wide temperature overview sufficient for first cut design decisions regarding permeability.

A linear permeability model, which represents the core by a parallel L-R circuit, is used to compute and interpret the magnetization properties from basic exciting winding current and induced voltage data, taken on bare toroidal cores. Related to this model, several figures of merit applicable to inductor materials are reviewed. In particular, the $\mu_r Q$ product figure of merit is shown to be proportional to the reciprocal specific core loss.

SAMPLE CORES

Unpackaged cores in several different categories were obtained from Vacuumschmeltze GmbH. They are representative of commercially available, competitive types and are not intended to be a specific endorsement.

The 6025F is a Co-based, relatively low saturation induction (B_s), very low core loss, high permeability, transverse magnetically annealed type, intended for fast pulse transformers and common mode chokes. The 6030F is also a Co-based, low core loss, transverse magnetically annealed material, but with a lower permeability, better linearity and a higher B_s. The 6030F is intended for power and pulse transformers that require a low remanent induction. The 500F is a partially recrystallized, Fe-based metallic glass of unspecified composition and anneal. Most likely it is similar to the Hitachi Metals, Ltd. *Finemet* alloy ($Fe_{73.5}Cu_1Nb_3Si_{13.5}B_9$) [2]. According to the manufacturer, the 500F is a low loss, high permeability, flat B-H loop material, having extra thermal stability and intended for high frequency inductor, transformer and common mode choke applications. Tape thicknesses and additional physical properties of the above materials are given in reference [4].

MEASUREMENT TECHNIQUE

Bare cores were placed in thin walled aluminum cases and data consisting of waveforms of the current in a primary exciting winding and induced voltage in a secondary sense winding were recorded by a digitizing oscilloscope. Further details of this standard type measurement setup are provided in reference [4].

REVIEW OF FIGURES OF MERIT

This section reviews a few simple measures of performance of a core material applicable to inductive elements, such as resonant energy storage and filter inductors. Their interpretation as figures of merit is application specific and hence can disagree on the benefit of a specific core property. For example, high μ materials can reduce the core size for a given inductance L, but they are simply not suitable for high current inductors because of magnetic saturation. As μ is increased, the coil winding volume and resistive losses will be reduced, but the total Q of the inductor will eventually be pulled down by the reduced Q of the core. The measures discussed below are tied to the experimental data by means of the parallel L–R circuit model outlined in Appendix A. Such large amplitude linear modeling can be accurate only for cores operating within a linear region of their B–H relation. Hysteresis and saturation obviously cause inaccuracies.

The main results of Appendix A are Equation (A14) for the relative permeability μ_r, Equation (A6) for the

quality factor Q of just the core material and Equation (A13) for the $\mu_r Q$ product figure of merit. These quantities are computable from the experimentally measured peak induced voltage V_p, peak exciting current I_p and either the total average power $\bar{P}_c$, or its core volume-specific version $\bar{p}_c$. Equation (A13) clearly shows that for given excitation conditions, the $\mu_r Q$ product measures the reciprocal specific core loss. Note that if the losses were classical eddy current, then $\bar{p}_c \propto f^2 B_p^2$ and $\mu_r Q \propto f^{-1}$.

For a given maximum useable B-field B_{max} of the material, as set by linearity requirements, the volume density $B_{max}^2 / (2\mu)$ of stored energy, is a measure of the merit of a core material to make up an inductor of a specified L to absorb voltage spikes. The basis for this is Equation (A20), which gives the the volt time area handling capability of an inductor. Its application requires caution, because the simple formula for L (Equation (A19)) shows that, for fixed core volume V_c and L, the $N / \bar{\ell}_c$ will increase as μ decreases. A large number of turns per unit mean length of the core can cause problems. For example, an inductor using a core material of very low μ_r, such as powdered iron or in the limit an air core, may require too thin a wire or have an unacceptably low total Q.

PERMEABILITY AND Q

Temperature resolved relative permeability (μ_r) data at 100 kHz is plotted for the 3 materials in Figures 1A, 1B and 1C. As may be expected for a linear B-H characteristic, the μ_r of these materials is not very sensitive to B_p, until saturation sets in. This is the interpretation suggested for the drooping with increasing temperature of some of the higher B_p curves for the 6025F and 6030F materials. It is very prominent in Figure 1A for the 6025F, which has the lowest Curie temperature T_c as well as the lowest B_s. These plots also suggest that the 500F is qualitatively different from the other two materials. The temperature sensitivity of the μ_r for the 500F is of opposite sign and bigger.

The f dependence of the μ_r of the 3 materials is presented in Figure 2, but at 0.10 T and 50 C only, due to project limitations. On a log-log scale, these plots seem to fit the shape seen in manufacturers' literature: a relatively flat low frequency region, going into rolloff as f increases and flattening again at high f. It is apparent too, that a full illustration of this behavior requires wider

frequency data than was obtained. The insensitivity of the 6030F μ_r to f in the 50 kHz to 1 MHz range should be noted for resonant inductor applications.

The f dependence of the 3 core materials Q is presented in Figure 3, but again only for 0.10 T at 50 C. Around and below 100 kHz, the curves drop rapidly with increasing frequency, reaching values less than unity in the case of the 500F and 6025F. Such surprisingly low values can be understood from the fact that the core Q is a composite of both magnetization and core loss properties, as both Equations (A6) and (A13) show. A high μ_r lowers the Q by lowering the stored energy for a given B_p. Moreover, a Q decreasing with increasing f at constant B_p, as seen in Figure 3, implies that the $\mu_r \overline{p}_c$ product grows faster than f.

SUMMARY AND CONCLUSIONS

100 kHz sinusoidal magnetization data was obtained over the temperature range of −150 C to 150 C for two amorphous and one partially recrystallized core materials. All of the selected materials have low magnetostriction (~ 0.2×10^{-6}) and a flat magnetization characteristic induced by transverse magnetic annealing. Each of these was picked to be representative of a class of commercial products:

1. A relatively low saturation (~0.5 T), cobalt based, amorphous tape, having very low losses and high permeability (~10^5 at low frequency). (Represented by type 6025F material.)

2. A higher saturation (~0.8 T), cobalt based, amorphous tape having low losses, a relatively low, but perhaps more temperature stable, permeability (~3×10^3) and a higher Curie temperature. (Represented by type 6030F material.)

3. A more recently developed, iron based, nanocrystalline tape, featuring some of the desirable soft magnetic properties of the cobalt based, amorphous tapes, but at a lower cost. (Represented by type 500F material.)

The low core loss characteristics of these materials are described over −150 C to 150 C in reference (4).

Magnetization properties of the core materials are described here by linear parameters based on a simple

parallel L-R circuit model of a core. Measures of performance, such as the relative permeability μ_r, the quality factor Q of the core material and the $\mu_r Q$ product are then derived from the data by using this model. At a given frequency and peak B-field, the $\mu_r Q$ product is proportional to the reciprocal specific core loss.

Temperature resolved relative permeability data at 100 kHz and selected peak B-fields (B_p) shows that the μ_r of these materials is not very sensitive to B_p, until saturation sets in. As may be expected for a linear B-H characteristic, the μ_r of these materials is not very sensitive to B_p, until saturation sets in. This is the interpretation suggested for the drooping with increasing temperature of some of the higher B_p curves for the Co-based materials. It is very prominent in Figure 1A for the 6025F, which has the lowest Curie temperature T_c as well as the lowest B_s. These plots also suggest that the 500F is qualitatively different from the other two materials. The temperature sensitivity of the μ_r for the 500F is of opposite sign and bigger.

A frequency (f) scan of the μ_r of the 3 materials, done only at 0.10 T and 50 C, shows on a log-log plot the usual flat low frequency region, followed by a rolloff as f increases and flattening again at high f. The μ_r of the 6030F type material is rather constant to at least 1 MHz, which can be valuable for resonant inductor applications.

Generally, none of the above materials are suitable to make up high Q, or high current inductors, unless cut and gapped to lower their permeability. The Q is already low at 100 kHz and drops rapidly with increasing f (Figure 3), reaching values less than unity in the case of the 500F and 6025F. Such low values can be understood from the fact that a high μ_r lowers the Q by lowering the stored energy for a given B_p. Unfortunately, gapping a tape wound core often leads to a remarkably increased core loss, concentrated near the cut faces. However, H. Fukunaga et al. [7] have shown that the introduction of thin ferrite pole face plates can still produce a superior inductor core by presumably reducing the in-plane eddy currents caused by the gap leakage B-field normal to the tape surfaces.

REFERENCES

1. G. Herzer and H.R. Hilzinger, "Recent Developments in Soft Magnetic Materials", Physica Scripta, vol. T24, 1988, pp. 22-28.

2. Y. Yoshizawa and K. Yamauchi, "Fe-Based Soft Magnetic Alloys Composed of Ultrafine Grain Structure", Materials Transactions, JIM, vol. 31, no. 4, April 1990, pp. 307-314.

3. G. Herzer and H.R. Hilzinger, "Surface Crystallization and Magnetic Properties in Amorphous Iron Rich Alloys", J. Magn. Magn. Mat., vol. 62, 1986, pp. 143-151.

4. J.M. Niedra and G.E. Schwarze, "Wide Temperature Core Loss Characteristics of Transverse Magnetically Annealed Amorphous Tapes for High Frequency Aerospace Magnetics", 34th Intersociety Energy Conversion Engineering Conference, Vancouver, BC, August 1999. Also NASA TM—209297.

5. W.R. Wieserman et al., "High Frequency, High Temperature Specific Core Loss and Dynamic B-H Hysteresis Loop Characteristics of Soft Magnetic Alloys", 25th Intersociety Energy Conversion Engineering Conference, Reno, NV, August 1990. Also NASA TM-103164.

6. V.J. Thottuvelil et al., "High-Frequency Measurement Techniques for Magnetic Cores", IEEE Power Electronics Specialists Conference, June 1985, pp. 412-425.

7. H. Fukunaga et al., "High Performance Cut Cores Prepared From Crystallized Fe-Based Amorphous Ribbon", IEEE Trans. Magn., vol. MAG-26, no. 5, September 1990, pp. 2008-2010.

APPENDIX A

<u>Linear Modeling of Core Magnetization Properties</u>

A magnetic core whose material is describable by a linear relation $B=\mu H=\mu_r\mu_0 H$, at least for $|B|<B_s$, can be modeled by linear circuit elements. Note, however, that hysteresis losses can not be modeled accurately this way. A parallel combination of inductance L_c and resistance R_c will be used here to represent the core. Hence for sinusoidal excitation, the relation between the voltage (or its time integral) across the L_c-R_c pair and the current into this pair is an ellipse. In the case of a time integrated voltage, this ellipse represents the apparent dynamic B-H hysteresis loop of the core. Any nonlinearity in the intrinsic B-H characteristic of the core material will be reflected as a distortion of the ellipse. Assuming negligible winding capacitance, the current measured in the exciting winding (N_1 turns) of a test core is the current into the L_c-R_c pair. And the voltage across this L_c-R_c pair is just (N_1/N_2) times the voltage sensed by a zero current secondary winding N_2.

<u>Equivalent circuit Q of magnetic core</u>

A general definition of the quality factor Q of an energy storing component is as 2π times the ratio of the peak stored energy to the energy dissipated per cycle. For an arbitrary impedance $\tilde{Z}$ (linear 2-terminal network), this can be shown to give

$$Q=\mathscr{I}m(\tilde{Z})/\mathscr{R}e(\tilde{Z}) \qquad (A1)$$

For an R_c in parallel with a reactance $X_c=\omega L_c$, one finds that

$$Q=R_c/X_c=R_c/(\omega L_c) . \qquad (A2)$$

The magnitude I_p of the peak current into this $\tilde{Z}_c$ is related to the magnitude V_p of the peak voltage across $\tilde{Z}_c$ by

$$I_p^2=(V_p/R_c)^2+(V_p/X_c)^2 . \qquad (A3)$$

Noting that $V_p=\sqrt{2}\,V_{rms}$, and also recognizing that $V_{rms}^2/R_c=\overline{P}_c$ is the total core loss, the relation (A3) can be rewritten into the form

$$(V_p I_p)^2=4(\overline{P}_c)^2+(V_p^2/X_c)^2 . \qquad (A4)$$

Division of Equation (A4) by $(2\overline{P}_c)^2$ then gives

$$(R_c/X_c)^2=\left(\frac{V_p I_p}{2\overline{P}_c}\right)^2-1 , \qquad (A5)$$

from which follows immediately that

$$Q=\left[\left(\frac{V_p I_p}{2\overline{P}_c}\right)^2-1\right]^{1/2} . \qquad (A6)$$

Equation A6 determines the core Q in terms of the measured total core loss $\overline{P}_c$ and the peak voltage and current. One can also show by applying trigonometric identities to the explicit voltage-current product time

function $v(t) \cdot i(t)$ that the $V_p I_p$ product is the same as the peak-to-peak value of $v(t) \cdot i(t)$:

$$V_p I_p = \left(v(t) \cdot i(t) \right)_{p-p} \quad . \tag{A7}$$

This is useful to estimate the limits to Q measurement imposed by instrument resolution, since $\overline{P_c} = \overline{v(t) \cdot i(t)}$.

Formula for the μQ product

A quick way to arrive at a formula for μQ (or $\mu_r Q$) is to combine the basic peak induced voltage formula

$$V_p = N_1 \omega A_c B_p \tag{A8}$$

with the inductive reactance formula

$$X_c = \omega L_c = \omega \mu N_1^2 A_c / \overline{\ell}_c \tag{A9}$$

such as to get

$$V_p^2 / X_c = \omega V_c B_p^2 / \mu \quad , \tag{A10}$$

where $V_c = \overline{\ell}_c A_c$ is the core volume. The V_p can be eliminated from Equation (A10), since

$$V_p^2 = 2 R_c \overline{P}_c \tag{A11}$$

relates it to the average total core loss $\overline{P}_c$. Recalling Equation (A2), this last step yields

$$Q = R_c / X_c = \omega B_p^2 / (2 \mu \overline{p}_c) \quad , \tag{A12}$$

where $\overline{p}_c = \overline{P}_c / V_c$. The $\mu_r Q$ product then is

$$\mu_r Q = \pi f B_p^2 / (\mu_0 \overline{p}_c) \quad . \tag{A13}$$

Relative permeability μ_r of the core material

Equation (A13) is immediately useful to get μ_r, because Q is available from Equation (A6). The result is

$$\mu_r \mu_0 = \omega B_p^2 / [(V_p I_p / V_c)^2 - 4 \overline{p}_c^2]^{1/2} \quad . \tag{A14}$$

Volt-time area handling capability

Let a periodic voltage $v(t)$ impressed across an inductance L be such that $v(t) > 0$ for $0 < t < t_1$ and $v(t) < 0$ for $t_1 < t < \tau$, where τ is the period. Also, $\overline{v(t)} = 0$ is assumed. Since $\overline{v(t)} = 0$, the $B(t)$ is periodic and may be assumed, without loss of generality, to swing between $-B_{max}$ and B_{max}, where $B_{max} > 0$. Integration of the magnetic induction law

$$v(t) = N \, d\phi/dt = N A_c \, dB/dt \tag{A15}$$

gives

$$\int_0^{t_1} v(t) \, dt = 2 N A_c B_{max} \tag{A16}$$

and

$$\int_{t_1}^{\tau} v(t) \, dt = -2 N A_c B_{max} \quad . \tag{A17}$$

Noting the polarity of $v(t)$, the above integrals can be combined in the form
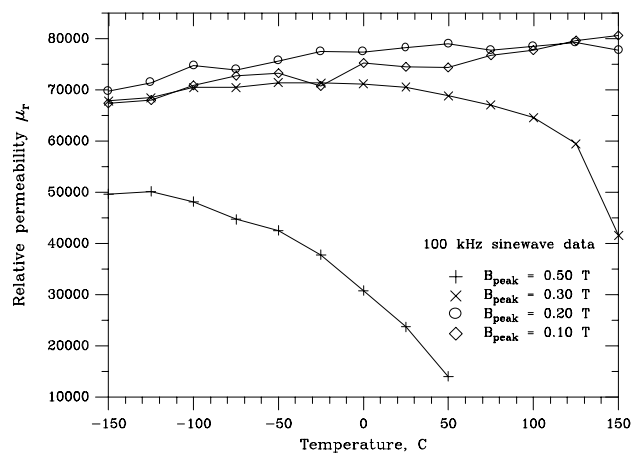
$$\int_0^{\tau} |v(t)| \, dt = 4 N A_c B_{max} \quad . \tag{A18}$$

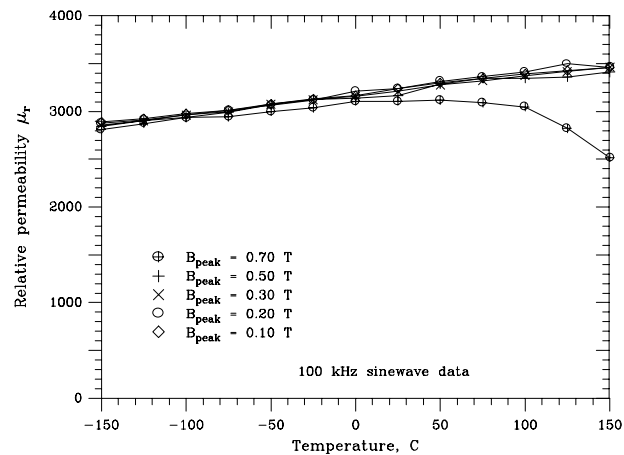The number of turns N can be eliminated from Equation (A18) by using the simple inductance formula

$$L = \mu N^2 A_c / \overline{\ell}_c = \mu (N / \overline{\ell}_c)^2 V_c \quad , \tag{A19}$$

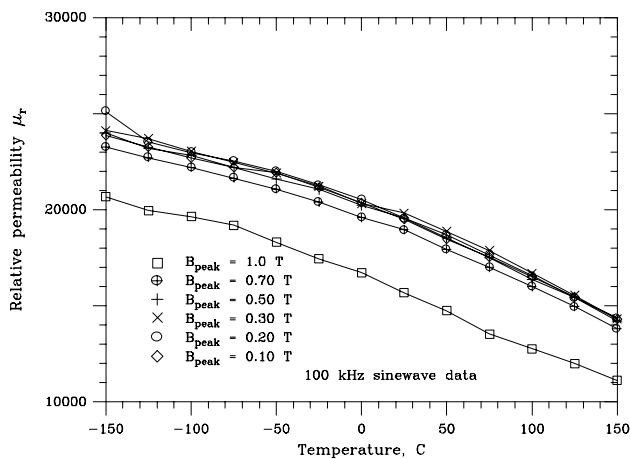which then puts Equation (A18) into the final form

$$\int_0^{\tau} |v(t)| \, dt = 4 B_{max} \, (L V_c / \mu)^{1/2} \quad . \tag{A20}$$

1A. Relative permeability of type 6025F Co−based amorphous tape.

1B. Relative permeability of type 6030F Co−based amorphous tape.

1C. Relative permeability of type 500F Fe−based nanocrystalline tape.

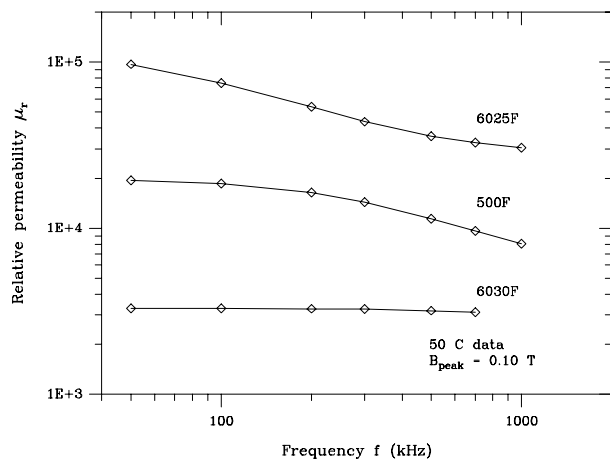Figure 1. Temperature dependence of the relative permeability at 100 kHz and selected values of B_{peak}.

Figure 2. Frequency dependence of the relative permeability of the 6025F, 6030F and 500F tape materials at 50 C and 0.1 T.
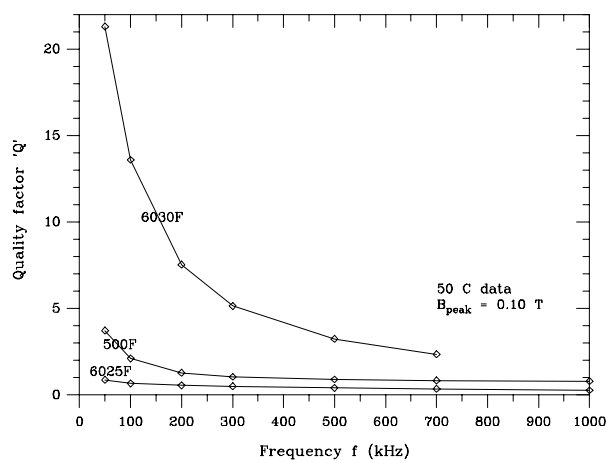

Figure 3. Frequency dependence of the quality factor 'Q' of the 6025F, 6039F and 500F tape materials at 50 C and 0.1 T.

REPORT DOCUMENTATION PAGE

1. AGENCY USE ONLY (Leave blank)	2. REPORT DATE	3. REPORT TYPE AND DATES COVERED
	August 1999	Technical Memorandum

4. TITLE AND SUBTITLE

Wide Temperature Magnetization Characteristics of Transverse Magnetically Annealed Amorphous Tapes for High Frequency Aerospace Magnetics

5. FUNDING NUMBERS

WU–632–1A–1C–00

6. AUTHOR(S)

Janis M. Niedra and Gene E. Schwarze

7. PERFORMING ORGANIZATION NAME(S) AND ADDRESS(ES)

National Aeronautics and Space Administration
John H. Glenn Research Center at Lewis Field
Cleveland, Ohio 44135–3191

8. PERFORMING ORGANIZATION REPORT NUMBER

E–11778

9. SPONSORING/MONITORING AGENCY NAME(S) AND ADDRESS(ES)

National Aeronautics and Space Administration
Washington, DC 20546–0001

10. SPONSORING/MONITORING AGENCY REPORT NUMBER

NASA TM—1999-209298

11. SUPPLEMENTARY NOTES

12a. DISTRIBUTION/AVAILABILITY STATEMENT

Unclassified - Unlimited
Subject Category: 33   Distribution: Nonstandard

This publication is available from the NASA Center for AeroSpace Information, (301) 621–0390.

12b. DISTRIBUTION CODE

13. ABSTRACT (Maximum 200 words)

100 kHz magnetization properties of sample transverse magnetically annealed, cobalt-based amorphous and iron-based nanocrystalline tape wound magnetic cores are presented over the temperature range of –150 C to 150 C, at selected values of B_{peak}. Frequency resolved characteristics are given over the range of 50 kHz to 1 MHz, but at $B_{peak} = 0.1$ T and 50 C only. Basic exciting winding current and induced voltage data were taken on bare toroidal cores, in a standard type measurement setup. A linear permeability model, which represents the core by a parallel L-R circuit, is used to interpret and present the magnetization characteristics and several figures of merit applicable to inductor materials are reviewed. The 100 kHz permeability thus derived decreases with increasing temperature for the Fe-based, nanocrystalline material, but increases roughly linearly with temperature for the two Co-based materials, as long as B_{peak} is sufficiently low to avoid saturation effects. Due to the high permeabilities, rather low values of the 'quality factor' Q, from about 20 to below unity, were obtained over the frequency range of 50 kHz to 1 MHz (50 C, $B_{peak} = 0.1$ T). Therefore these cores must be gapped in order to make up high Q or high current inductors. However, being rugged, low core loss materials with flat B-H loop characteristics, they may provide new solutions to specialty inductor applications.

14. SUBJECT TERMS

Magnetic material; Magnetic permeability; Quality factor Q; Amorphous material; Nanocrystalline material; Wide temperature; High frequency

15. NUMBER OF PAGES
12

16. PRICE CODE
A03

17. SECURITY CLASSIFICATION OF REPORT	18. SECURITY CLASSIFICATION OF THIS PAGE	19. SECURITY CLASSIFICATION OF ABSTRACT	20. LIMITATION OF ABSTRACT
Unclassified	Unclassified	Unclassified	